

AMO inversion to a common azimuth dataset

Robert G. Clapp¹

ABSTRACT

I cast 3-D data regularization as a least-squares inversion problem. The model space is a four-dimensional $(t, \text{cmp}_x, \text{cmp}_y, h_x)$ hypercube. An interpolation operator maps to an irregular five dimensional space $(t, \text{cmp}_x, \text{cmp}_y, h_x, h_y)$ which is then mapped back into a four dimensional space by applying Azimuth Move-Out (AMO). A regularization term minimizes the difference between various $(t, \text{cmp}_x, \text{cmp}_y)$ cubes by applying a filter that acts along offset. AMO is used to transform the cubes to the same h_x before applying the filter. The methodology is made efficient by Fourier-domain implementation and pre-conditioning of the problem. I apply the methodology on a simple synthetic and to a real marine dataset.

INTRODUCTION

The irregularity of seismic data, particularly 3-D data, in both the model domain (in terms of subsurface position and reflection angle) and the data domain (in terms of midpoint, offset, and time) cause imaging problems. Migration methods desire a greater level of regularity than is often present in seismic surveys. There are two general approaches to deal with this problem. One approach is to treat the imaging problem as an inverse problem. The migration operator can be thought of as a linear transform from the recorded data to image space. Ronen and Liner (2000); Duquet and Marfurt (1999); Prucha et al. (2000) use the migration operator in a linear inverse problem to overcome irregular and limited data coverage. A regularized that encourages consistency over reflection angle is used to stabilize the inverse. These approaches have shown promise but are generally prohibitively expensive, and rely on an accurate subsurface velocity model.

Another approach is to try to regularize the data. AMO provides an effective regularization tool (Biondi et al., 1998) and is generally applied as an adjoint to create a more regularized volume. These regularized volumes still often contain in ‘acquisition footprint’ or more subtle amplitude effects. Chemingui (1999) used a log-stretch transform to make the AMO operator stationary in time. He then cast the regularization problem as a frequency-by-frequency inversion problem using a Kirchoff-style AMO operator. He showed that the acquisition footprint could be significantly reduced. The downside of this approach is the relatively high cost of Kirchoff implementation of AMO.

¹email: bob@sep.stanford.edu

Biondi and Vlad (2001) built on the work of Fomel (2001) and set up an inverse problem relating the irregular input data to a regular model space. They regularized the problem by enforcing consistency between the various $(t, \text{cmp}_x, \text{cmp}_y)$ cubes. The consistency took two forms. In the first, a simple difference between two adjacent in-line offset cubes was minimized. In the second, the difference was taken after transforming the cubes to the same offset AMO. Clapp (2005b) set up the data regularization with AMO as an inverse problem creating a full volume $(t, \text{cmp}_x, \text{cmp}_y, h_x, h_y)$.

In this paper, I modify the approach of Clapp (2005b) so that the model space is a common azimuth volume. I introduce an additional mapping operator that maps from the full $(t, \text{cmp}_x, \text{cmp}_y, h_x, h_y)$ to $h_y = 0$ using AMO. In addition, I show that the combination of limited h_y and consistent coverage as a function of h_x in marine surveys can still produce undesired amplitude variation as a function of cmp_y . To solve this problem, I introduce an additional regularization term that creates consistency as a function of cmp_y .

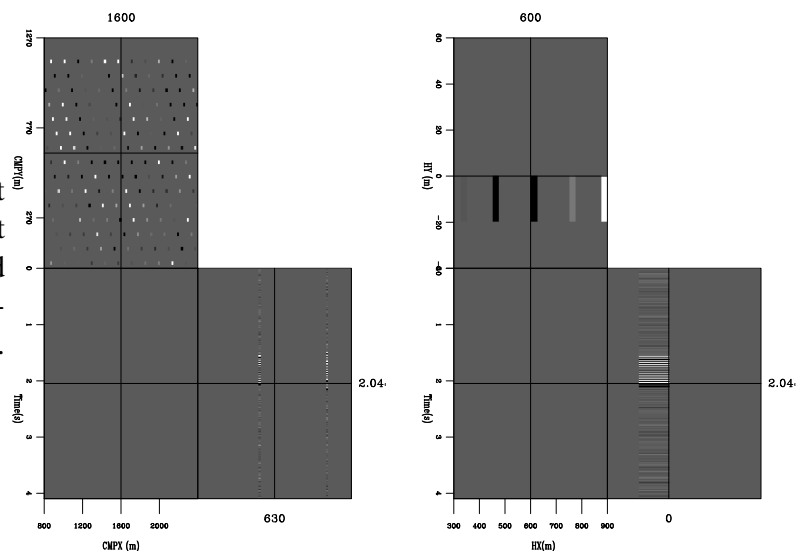
THEORY

Estimating a regularly sampled common-azimuth volume \mathbf{m} from our irregular input data \mathbf{d} can be set up as a least squares inversion problem. In this section, I will go over an approach to create a common azimuth volume by setting up an inverse problem. I will use a small synthetic to demonstrate the need for the various operators in the inversion process.

The data consists of irregular traces in a 5-D space $(t, \text{cmp}_x, \text{cmp}_y, h_x, h_y)$. The AMO operator acts on regularly sampled $(t, \text{cmp}_x, \text{cmp}_y)$ cubes, so we map from the irregular data space to the regular model space using a simple linear interpolation operator \mathbf{L} . Figure 1 shows two cube views from the five dimensional space the data is mapped into. Notice the sparseness of the data in these cubes. In standard marine acquisition, a single cross-line offset is acquired for each midpoint. The standard multi-streamer acquisition results in variation of the cross-line offset that is filled as we scan over cmp_y .

Figure 1: The location of the input traces for a simple synthetic. The left panel is a constant offset cube (fixed h_x and h_y). The right panel is a single midpoint (fixed cmp_x and cmp_y).

`bob1-interp` [CR,M]



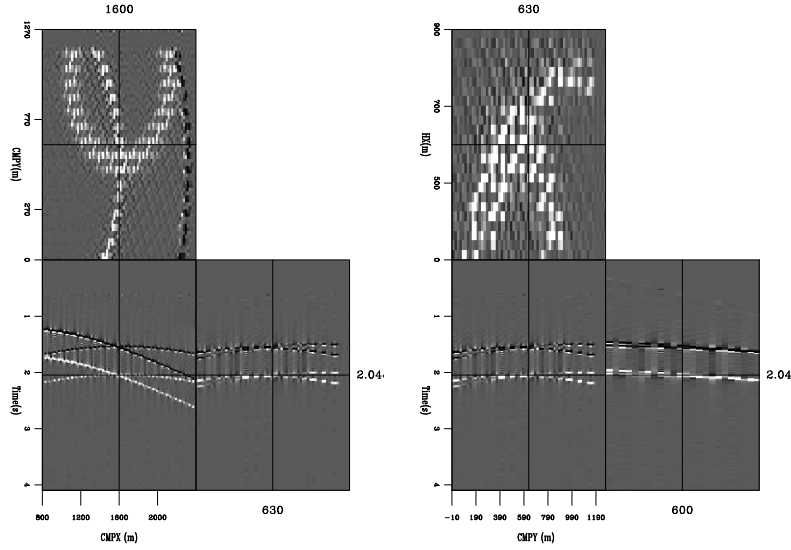


Figure 2: The result of applying \mathbf{Z} to the data shown in Figure 1. The left panel shows three slice from constant offset cube. The right panel shows three slice from a constant cmp_y cube.

`bob1-zero` [CR,M]

For common azimuth migration, we want all of our data to reside at $h_y = 0$. As a result, we need to use AMO to transform from the h_y that the data was recorded at to $h_y = 0$. The operator \mathbf{Z}' is a sum over the $(t, \text{cmp}_x, \text{cmp}_y)$ cubes that have been transformed to $h_y = 0$. Figure 2 shows two cube views of the result of applying \mathbf{Z}' to the small synthetic. In this case we still have significant holes along cmp_y . I will discuss why I created these holes later in the section.

Finally, we need to add in our regularization term. Generally, after NMO, our data should be smooth as a function of offset. We can think of adding a derivative operator along the offset axis. We can improve this estimate even further by applying a derivative on cubes that have been transformed to the same offset using $\text{AMO}^2 \mathbf{D}_h$. We can write our fitting goals as

$$\begin{aligned} \mathbf{d} &\approx \mathbf{LZm} \\ \mathbf{0} &\approx \epsilon \mathbf{D}_h \mathbf{m}, \end{aligned} \quad (1)$$

where ϵ controls the importance of consistency along the offset axis. We can speed up the convergence of this problem by preconditioning the model with the inverse of our regularization operator. In this case, we replace taking the derivative of AMO cubes with performing causal integration of AMO cubes \mathbf{C}_h . Our new fitting goals then become

$$\begin{aligned} \mathbf{d} &\approx \mathbf{LZC}_h \mathbf{p} \\ \mathbf{0} &\approx \epsilon \mathbf{p}, \end{aligned} \quad (2)$$

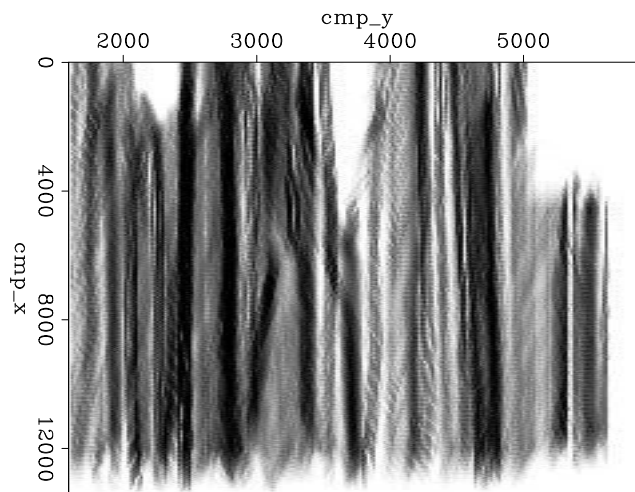
where $\mathbf{m} = \mathbf{C}_h \mathbf{p}$.

²In this case AMO simplifies to Dip Move-out because it is being applied simply along the h_x axis

Large holes

This set of fitting goals can run into problems when we deal with real marine geometry. To demonstrate the problem we will look at where data was recorded for a real 3-D marine survey. We can calculate where we have traces in the $h_x, \text{cmp}_x, \text{cmp}_y$ plane. If our acquisition lines are perfectly straight, we are able to acquire data throughout our survey. If our grid is perfectly oriented with acquisition geometry, we should have consistent fold in this cube. Figure 3 shows that this is far from the case. The figure shows the result of stacking over all offsets. Note that we have some areas where we don't have any data (white). If we use fitting goals (2) to estimate our model we run into a problem. The inversion result will show a dimming of amplitudes as we move away from our known data. Figure 5 shows the result of applying

Figure 3: Fold of a real marine dataset. Note how we have some regions with zero fold (white). `bob1-fold` [CR]



fitting goals (2) to our synthetic. Note how the amplitude declines markedly as we move away from locations where we have data. Even more problematic than dimming is when we see significant unrealistic, brightening of amplitudes for certain cmp_y . The brightening is caused by the fold pattern seen in Figure 4. The three panels represent the fold in the $(\text{cmp}_x, \text{cmp}_y)$ plane as we increase in offset from left to right. Note how we have fairly regular coverage at the near offsets and much more variable coverage as we move to larger offsets. This inconsistency is mainly caused by cable feathering. For some cmp_y we only have near offset traces. The near offset traces tend to be of higher amplitude and are more consistent as function of h (the tops of hyperbolas are insensitive to velocity errors). Our model covariance operator puts these unrealistically large amplitudes at all offsets, resulting in a striping of the amplitudes as a function of cmp_y .

Both of these problems are due to the lack of ‘mixing’ of information along the y direction. By mixing I mean that a column of the matrix implied by fitting goals (2) has very few non-zero elements at cmp_y 's different from the cmp_y associated with its corresponding model point. Our regularization is just DMO, which produces no mixing in the y direction. Our zeroing operator produces a limited amount of mixing, but the range is limited due to the small offset in the h_y direction inherent in marine surveys. As a result our inversion can have realistic kinematic but unrealistic amplitude behavior as a function of cmp_y . A simple solution to this problem is to introduce another operator to our model covariance description that tends to

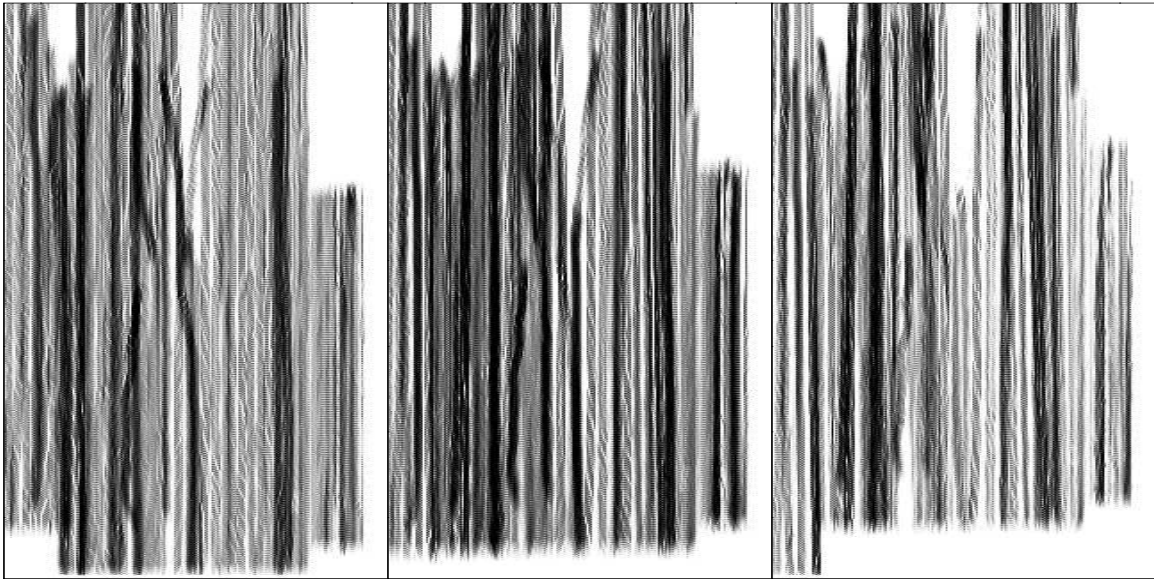


Figure 4: The three panels represent the fold in the (cmp_x, cmp_y) plane as we increase in offset from left to right. Note how we have fairly regular coverage at the near offsets and much more variable coverage as we move to larger offsets. For some cmp_y we only have near offset traces.

`bob1-fold-off` [CR]

produce consistency as a function of cmp_y . We must be careful to avoid introducing unrealistic smoothness in the cmp_y direction by our choice of preconditioners. I chose leaky integration along the cmp_y plane \mathbf{B}_y . The leaky integration will encourage the inversion to keep consistent amplitudes unless the data says otherwise. Using a relatively small leaky parameter and a very small ϵ should force it to have only an amplitude balancing effect rather than an effect on the kinematics of the solution.

Combining our two model preconditioners we get a new operator \mathbf{S} ,

$$\mathbf{S} = \mathbf{C}_h \mathbf{B}_y, \quad (3)$$

and a new set of fitting goals

$$\begin{aligned} \mathbf{d} &\approx \mathbf{LZSp} \\ \mathbf{0} &\approx \epsilon \mathbf{p}. \end{aligned} \quad (4)$$

Figure 6 shows the result of applying fitting goals (4) to the small synthetic. Note how the amplitude behavior is much more consistent than the result shown in Figure 5.

Fitting goals (4) should be avoided when possible. They introduce a smoothing along the cmp_y axis that is often unrealistic. Unfortunately when encountering large acquisition holes, some additional regularization is needed.

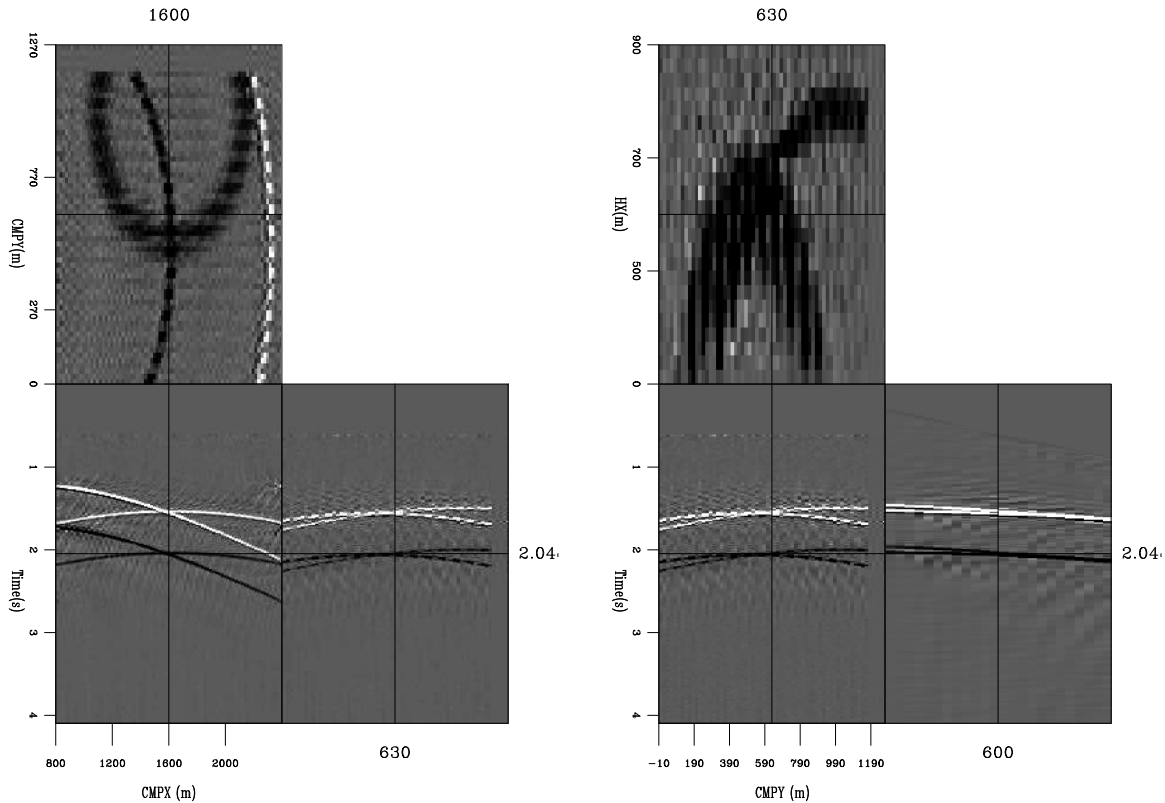


Figure 5: Two views of the result of applying fitting goals (2). The left panel is a three dimensional view at a fixed h_x . The right panel is a three dimensional view at a fixed cmp_x . Note the inconsistent, unrealistic amplitude behavior as a function of cmp_y . bob1-bad-syn [CR,M]

IMPLEMENTATION

A cost-effective implementation of fitting goals (2) or (4) is challenging. The obvious domain to parallelize the inversion is over frequency. In this case the model and data's time axis is log-stretched and transformed into the frequency domain. The resulting model and data space are approximately three times their time domain representation due to the oversampling necessitated by the log-stretch operation. In addition, both these volumes need to be transposed. To apply the log-stretch FFT operation, the natural ordering is for the time/frequency axis to be the inner axis while the inversion is more efficient with the time/frequency axis being the outer axis. An out-of-core transpose grows in cost with the square of the number of elements. For efficiency, I do a pre and post-step parallel transpose of the data in conjunction with the transformation to and from the log-stretched frequency domain. I split the data long the cmp_y axis. For the pre-step I log-stretch and FFT the input data, I then do an out-of-core transpose of this smaller volume. I then collect the transposed data. The post-step operation is simply the inverse, transpose and then FFT and unstretch.

A second major problem is the number of iterations necessary for convergence. The causal

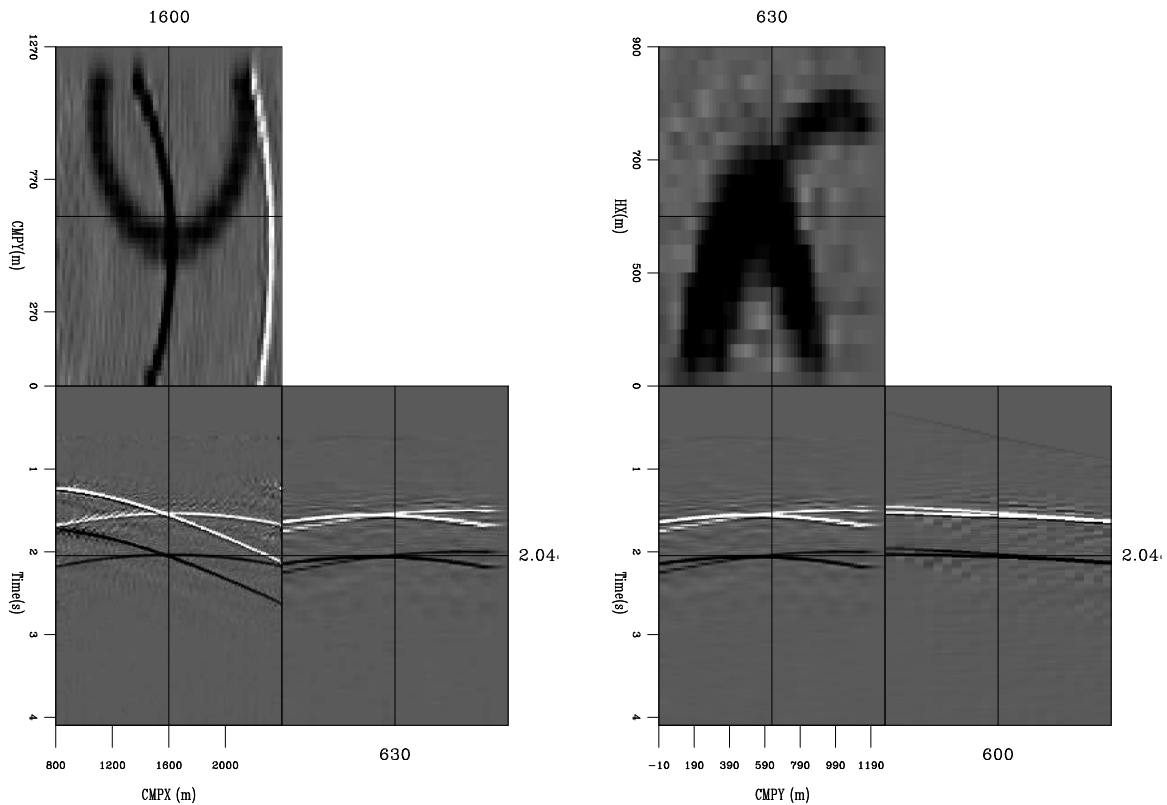


Figure 6: Two views of the result of applying fitting goals (4). The left panel is a three dimensional view at a fixed h_x . The right panel is a three dimensional view at a fixed cmp_x . Both views are identical the ones shown in Figure 5. Note how the unrealistic amplitude behavior seen in Figure 5 has been corrected. `bob1-inv-syn` [CR,M]

integration and leaky integration are good preconditioners (fast convergence) but the AMO portion tends to slow the inversion. As a result many (20-100 iterations) are desirable. The global inversion approach described in Clapp (2005b) is IO dominated. It also relies on hardware stability. Both of these factors make a frequency-by-frequency in-core inversion non-ideal but better choice. The major drawback to a frequency by frequency approach is that the frequencies might converge at significantly different rates resulting in an image that is unrealistically dominated by certain frequency ranges (most likely the low). To minimize this problem, I stopped the inversion after a set reduction in the data residual.

The final issue is the size of the problem. The domain of \mathbf{L} is four-dimensional and can be quite large even for a relatively small model space. In addition, for a conjugate gradient approach we still must keep three copies of our data space (data, data residual, previous step data residual) and five copies of our model space (gradient, model, previous step, previous step model residual, model residual). As a result, we need a machine with significant memory and/or break the problem into patches in the (cmp_x, cmp_y) plane.

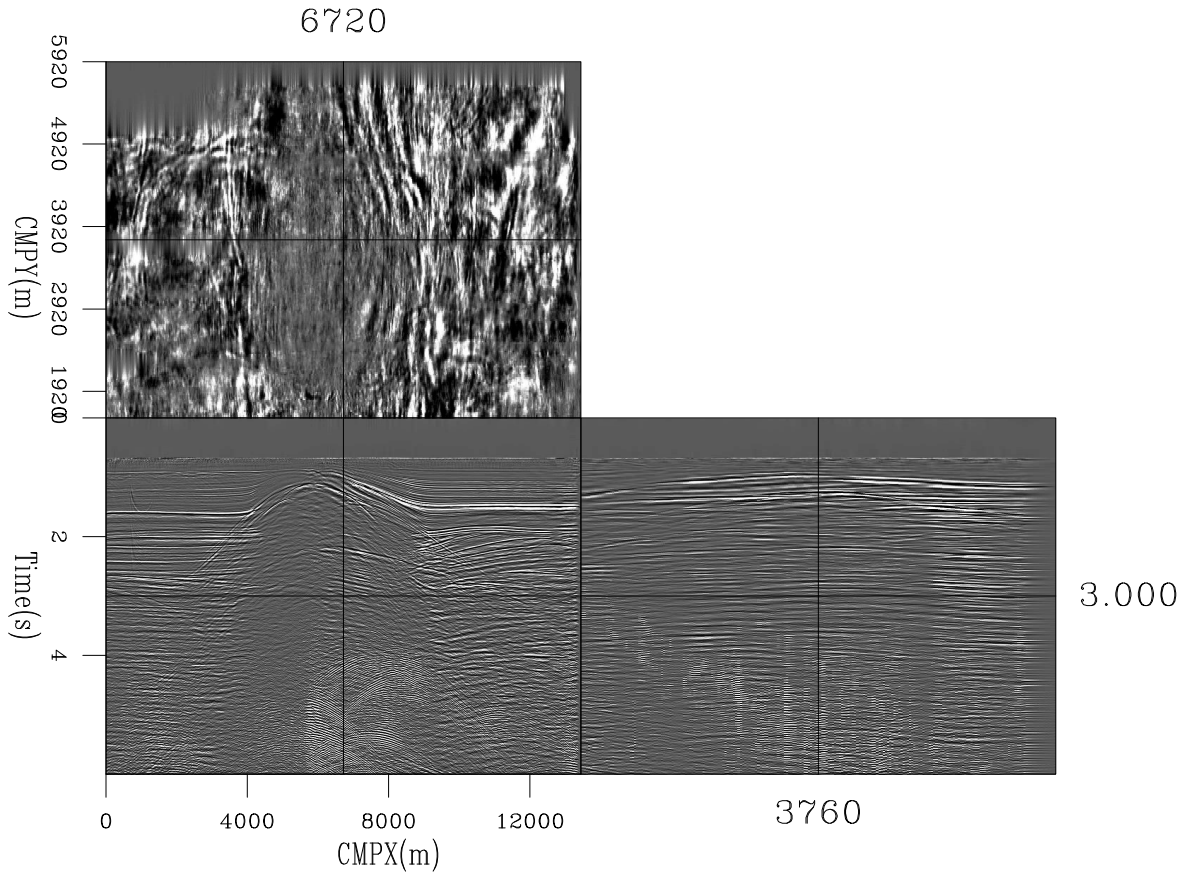


Figure 7: A constant offset section from a real 3-D marine dataset obtained by applying fitting goals (4). Note the absence of an acquisition footprint. `bob1-const-off` [CR]

REAL DATA EXAMPLE

I tested the methodology on a real 3-D marine dataset from the North Sea. Figures 3 and 4 are from this dataset. Previous uses of AMO and common azimuth migration have resulted in noticeable acquisition footprint in the first 1000 meters (Biondi, 1999; Vaillant and Sava, 1999). For the test I used a maximum of 40 iterations, with a maximum reduction in residual of 35%. A large reduction would be preferable but many frequencies did not reduce by even 20% after 40 iterations. Figure 7 shows a constant offset section after regularization with fitting goals (4). Note the absence of an acquisition footprint. Further, note how we have successfully filled even the large hole visible in the fold map of Figure 3.

I then applied common azimuth migration to the data. Figure 8 show three slices from the zero-offset migration cube. Pay particular attention to the depth slice. Note how the acquisition footprint has disappeared.

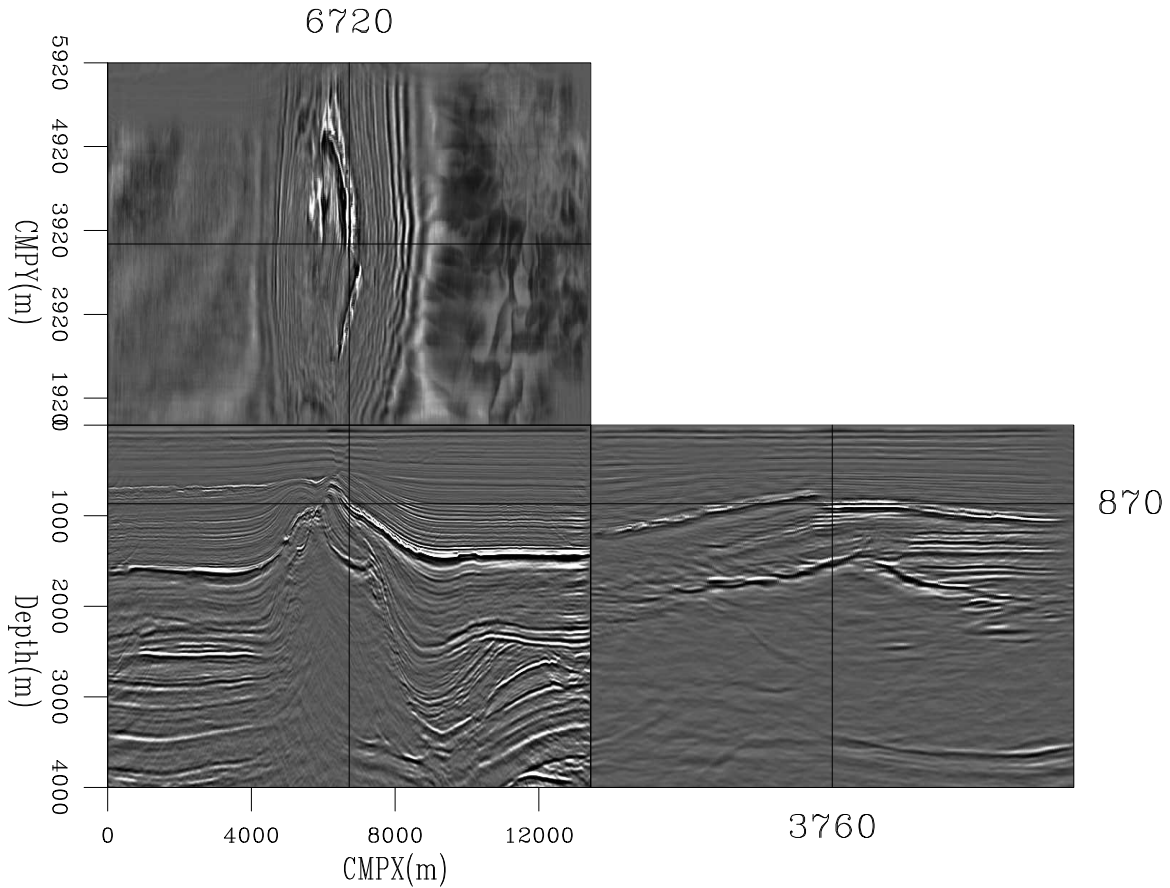


Figure 8: The result of migrating the data show in Figure 7. Note that virtually no acquisition footprint is visible in the data. `bob1-mig` [CR]

FUTURE WORK

The decay in the residual varies significantly as a function of frequency. At most frequencies the residual decreases only 40% between the first and 40th iteration. It appears that the large values in the residual are dominated by events at the cusp of the mute zone. Clapp (2005a) faced similar problems when inverting for an image using migration as her linear operator. Introducing a weight function in the frequency domain has the potential to speed up the inversion of both problems.

CONCLUSION

An inversion method to produce a dataset appropriate for common azimuth migration is introduced. The inversion problem uses AMO to both map the data to a constant $h_y = 0$ and as part of regularization operator to assure consistency between (cmp_x, cmp_y, hx) cubes.

ACKNOWLEDGMENTS

I would like to thank TotalFinaElf for providing the data used in this paper.

REFERENCES

- Biondi, B., and Vlad, I., 2001, Amplitude preserving prestack imaging of irregularly sampled 3-D data: *SEP-110*, 1–18.
- Biondi, B., Fomel, S., and Chemingui, N., 1998, Azimuth moveout for 3-D prestack imaging: *Geophysics*, **63**, no. 2, 574–588.
- Biondi, B. L., 1999, 3-D Seismic imaging: Stanford Exploration Project.
- Chemingui, N., 1999, Imaging irregularly sampled 3D prestacked data: *SEP-101*.
- Clapp, M. L., 2005a, Imaging under salt: illumination compensation by regularized inversion: Ph.D. thesis, Stanford University.
- Clapp, R. G., 2005b, Data regularization: Inversion with azimuth move-out: *SEP-120*, 187–196.
- Duquet, B., and Marfurt, K. J., 1999, Filtering coherent noise during prestack depth migration: *Geophysics*, **64**, no. 4, 1054–1066.
- Fomel, S., 2001, Three-dimensional seismic data regularization: Ph.D. thesis, Stanford University.
- Prucha, M. L., Clapp, R. G., and Biondi, B., 2000, Seismic image regularization in the reflection angle domain: *SEP-103*, 109–119.
- Ronen, S., and Liner, C. L., 2000, Least-squares DMO and migration: *Geophysics*, **65**, no. 5, 1364–1371.
- Vaillant, L., and Sava, P., 1999, Common-azimuth migration of a North Sea dataset: *SEP-102*, 1–14.